Chapter 1

An Unfolding Theory Approach to Bursting in Fast-Slow Systems

Martin Golubitsky
University of Houston

Krešimir Josić and Tasso J Kaper
Boston University

Many processes in nature are characterized by periodic bursts of activity separated by intervals of quiescence. In this chapter we describe a method for classifying the types of bursting that occur in models in which variables evolve on two different timescales, i.e., fast-slow systems. The classification is based on the observation that the bifurcations of the fast system that lead to bursting can be collapsed to a single local bifurcation, generally of higher codimension. The bursting is recovered as the slow variables periodically trace a closed path in the universal unfolding of this singularity. The codimension of a periodic bursting type is then defined to be the codimension of the singularity in whose unfolding it first appears. Using this definition, we systematically analyze all of the known universal unfoldings of codimension-one and -two bifurcations to classify the codimension-one and -two bursters. Takens was the first to analyze the unfolding spaces of a number of these. In addition, we identify several codimension-three bursters that arise in the unfolding space of a codimension-three degenerate Takens-Bogdanov point. Among the periodic bursters encountered in mathematical models for nerve cell electrical activity, so-called elliptical, or type III, bursters are shown to have codimension two. Other bursters studied in the literature are shown to first appear in the unfolding of the degenerate Takens-Bogdanov point and thus have codimension three. In contrast with previous classification schemes, our approach is local, provides an intrinsic notion of complexity for a bursting system, and lends itself to numerical implementation.

1.1 A framework for classifying bursters

The fields of mathematical and computational neuroscience focus on modeling electrical activity in nerve cells. Fundamental processes, such as voltage changes and ion transport across cell membranes, occur on disparate time scales. As a result, the mathematical models consist of fast and slow variables:

$$\begin{aligned} x' &= f(x,y) \\ y' &= \epsilon g(x,y) \end{aligned} \tag{1.1}$$

where $\epsilon > 0$ is small.

The Hodgkin-Huxley equations, FitzHugh-Nagumo equations, Morris-Lecar equations, as well as many other fast-slow models of the above form, exhibit an extremely rich variety of nonlinear dynamical behaviors. In this work, we focus exclusively on the phenomenon of periodic bursting.

Rinzel [52] defines a periodic *burster* as a periodic solution to a system of autonomous differential equations whose behavior alternates between near steady-state and trains of approximate spike-like oscillation; see also [66]. Within the particular framework of fast slow systems (1.1), Rinzel [50, 51, 54], Ermentrout and Kopell [23] and others, use analytical methods for identifying and constructing periodic bursters. One thinks of the slow variables y as providing a time-periodic forcing in the fast x' equation, so that the solution of the fast equation visits various invariant sets in order. As noted in [54], the slow variables either provide this forcing effectively *without* feedback from the fast system, in which case the slow variables oscillate periodically on their own, irrespective of how the coupling to the fast subsystem influences them. Or, they provide it *with* feedback from the fast system, in which case the switching between the two states is determined also by the fast variables.

In the former case, the system may effectively be modeled as:

$$\begin{aligned} x' &= f(x,y) \\ y' &= \epsilon g(y) \end{aligned} \tag{1.2}$$

with the slow component only depending on the slow variable y. A reduction to (1.2) can also be made for the latter case. However, in this second case, one needs to use invariant manifold theory, and the reduction is made separately over each of the local segments of the periodic trajectories, not globally over the entire period of the slow oscillation.

There is also a geometric approach to constructing bursters that entails thinking of bursters as generalized heteroclinic orbits. Here the bursting trajectory is a trajectory that moves from one invariant set (a steady state, a periodic solution, or a quasiperiodic solution) to another, spending a relatively short time in transition and a relatively long time near each invariant set. Golubitsky and Stewart [28] emphasized the heteroclinic structure of bursters by introducing the stylized notion of a pipe system in phase space. Pipe systems consist of joints containing hyperbolic invariant sets, such as equilibria and limit cycles, and tubes connecting the joints. They showed that primitive piecewise smooth constructions of pipe systems do lead to bursting time series of the type seen in experiments.

From all of these points of view, a bursting trajectory is described by certain characteristics: the sequence of invariant states (equilibria, periodic orbits, invariant tori, etc.) visited by the bursting trajectory and the ways in which these trajectories approach and leave each invariant set. The classification schemes that have been explored based on such phenomenological descriptions, including that in Izhikevich [37], all suffer from one difficulty — there is no way to know when the classification is complete.

In this chapter, we suggest that bursters should be classified by their phenomenological description *and* by the codimension of the singularity in whose unfolding they first appear. We will use the fast slow structure in (1.2) and the local unfolding ideas as a basis for this classification scheme. This approach is analogous to the path formulation description of bifurcation problems given in [26] where here the paths will be closed curves rather than curves and the unfolding theory will be the dynamical systems unfolding theory described in [30] rather than the singularity theory unfolding theory of Thom and Mather.

This local approach has several advantages over the above global analytical and geometrical methods. First, it is well known [20, 26, 27, 30] that many bifurcations that are first observed globally can be more easily studied by local theory, i.e., by using the unfolding theory of degenerate singularities. In particular, the local theory provides methods by which global phenomena can be found locally using calculus and numerical techniques. Second, the local theory provides a rational method of classification by codimension that naturally indicates how complex a system needs to be in order for it to support bursters of given types.

The local approach developed in this work based on the unfolding of singularities may be viewed as a logical extension of the approach taken in Bertram *et al.* [8]. In particular, Bertram *et al.* [8] showed that the distinct bursters known at the time, including the three from the classification of [51], as well as some found later, could be obtained by choosing appropriate paths in the bifurcation diagram of a codimension-three degenerate Takens-Bogdanov bifurcation point. Their analysis, in turn, relied heavily on the results reported in Dumortier *et al.* [22] for the unfolding space of this singularity. The central new element we add is that the codimension of a periodic bursting type should be the codimension of the singularity in whose unfolding the burster first appears. It is this new definition, made precise in definition 1.5 below, that makes possible a rational classification scheme and that offers a natural measure of the complexity of each bursting type.

Our work also complements the classification scheme presented in de Vries [67]. There, a bifurcation map of the parameter space is developed by first finding the codimension-one bifurcation curves and then by finding the special codimension-two points along these curves that bound the regions with different bursters. The domain of the map is naturally split into separate regions, one for each distinct bursting type. This map therefore broadens the schemes developed earlier in [51] and [8].

Remark 1.1. The need for a cogent mathematical classification also stems from the fact that there are difficulties inherent in relating features of times series to the topological classifications of bursters; see [8] and [37]. In particular, indicators from the time series, such as phase resetting, spike-frequency profiles, and spike undershoot, only provide a limited tool for classification.

1.1.1 Phenomenological Approach to Bursting in Fast-Slow Systems

A necessary condition for bursting in (1.2) is that each of the fast system invariant sets must be asymptotically stable for certain values of y and lose stability at a bifurcation as y changes. Assuming that the slow system is varying periodically, which we assume for periodic bursters, we can rewrite (1.2) as a periodically forced system of differential equations of the form

$$x' = f(x, y(\epsilon t)). \tag{1.3}$$

We now think of the solution of (1.3) as visiting invariant states of the frozen system

$$x' = f(x, y^*) \tag{1.4}$$

where $y^* = y(\theta)$ for some θ. i.e., the time-periodic evolution of $y(t)$ forces the solution trajectory $x(t)$ to oscillate between these invariant sets. With this structure in mind, we define a burster type as follows.

Definition 1.2. A periodic burster *type* consists of

(a) an ordered set S_j $(j = 1, \ldots, \ell)$ of stable equilibria, periodic orbits, or invariant tori for the frozen system (1.4) existing at $y^* = y(\theta)$ for θ in the interval (θ_j, θ_{j+1}), where $\theta_{\ell+1} = \theta_1$.
(b) the type of bifurcation that S_j undergoes as θ varies past θ_{j+1}, where these bifurcations cause the trajectory to leave the vicinities of the invariant sets.
(c) the eigenvalues (or spectra) — all real (nodal) or some complex (oscillatory) — associated to each S_j.

We assume that the eigenvalues (or spectra) of S_j in (c) do not change their type as θ varies in (θ_j, θ_{j+1}) nor do the signs of their real parts change.

Remark 1.3. This definition of bursting allows for bursting in systems in which there is at most one stable state at each parameter value of the fast system. Hence, it contrasts with previous descriptions of bursters which rely primarily on bistability of states. Furthermore, our description of bursters leads to an enlargement of the class of systems that are labeled as 'bursting'. For example, it includes bursts between two steady states, which have no spiking in the active phase.

1.1.2 A Local Description Using Singularities and Their Unfoldings

We now set up our framework for discussing the local birth of periodic bursters. We assume that the frozen system

$$x' = f(x, 0)$$

has a singularity of codimension k at $x = 0$ and that the y variables are universal unfolding parameters for this singularity. That is, we assume that $f : \mathbb{R}^n \times \mathbb{R}^k \to \mathbb{R}^n$. In this context, we assume that the unfolding theorem is valid and $y(\theta)$ is a small amplitude periodic path in $\mathbb{R}^k$. Of course, our discussion only refers to an unspecified neighborhood of the origin in $\mathbb{R}^k$, so that the convention of writing the parameter space of k parameters as $\mathbb{R}^k$ is a slight abuse of notation.

Locally, near the origin the universal unfolding defines a codimension-one transition variety $\mathcal{V} \subset \mathbb{R}^k$. This variety consists of parameter values at which singularities of codimension at least one occur. These singularities include, but are not limited to, saddle-node bifurcations, Hopf bifurcations, and homoclinic trajectories.

A diffeomorphism $\varphi : \mathbb{R}^k \to \mathbb{R}^k$ *preserves* $\mathcal{V}$ if $\varphi(\mathcal{V}) = \mathcal{V}$ and if it maps each component manifold constituting the variety to itself. Hence, in particular, it is the case that $\varphi(0) = 0$ whenever φ preserves $\mathcal{V}$, since 0 is the only codimension-k point of $\mathcal{V}$.

Definition 1.4. Two paths $y(\theta)$ and $z(\theta)$ are *path equivalent* if there exists a map $\varphi : \mathbb{R}^k \times \mathbf{S}^1 \to \mathbb{R}^k$ and a reparametrization $\Theta : \mathbf{S}^1 \to \mathbf{S}^1$ such that $\varphi(\cdot, \theta)$ is a diffeomorphism that preserves $\mathcal{V}$ for each $\theta \in \mathbf{S}^1$ and

$$z(\theta) = \varphi(y(\Theta(\theta)), \theta).$$

Therefore, one directly sees that whenever $y(\theta)$ and $z(\theta)$ are path equivalent, the corresponding bursters have the *same type.* The idea is that when two paths are path equivalent they traverse the same sets of (stable) equilibria, periodic solutions, etc. with the same eigenvalue types — hence they have the same burster types.

1.1.3 Classification Based on Minimum Codimensions of Singularities

We make the following definition of codimension of a periodic bursting type in order to be able to classify periodic bursters in a framework intrinsic to the fast-slow decomposition of the governing equations. The viewpoint adopted here is that, among all of those singularities whose unfoldings contain a given bursting type, the one with smallest codimension gives an intrinsic measure of the complexity of that burster:

Definition 1.5. The *codimension* of a periodic bursting type is the minimum codimension of a bifurcation point in the fast system in whose unfoldings that type of bursting occurs.

Definition 1.5 forms the basis for the classification presented in this work. We will show that there is a single codimension-one burster, namely that which arises through a (nondegenerate) Hopf bifurcation in the fast subsystem. Then, we classify all codimension-two bursters by systematically studying the known unfoldings of all codimension-two bifurcations. These include: the cusp singularity, degenerate Hopf bifurcation, Takens-Bogdanov bifurcation, Hopf-steady state mode interaction, and Hopf-Hopf mode interaction. All other bursting types must be of codimension three or more, and in this work we will also discuss certain codimension-three bursters.

A surprising observation resulting from our analysis is that systems traditionally labeled as type III (or elliptic) bursters have codimension two, whereas the other most commonly studied bursters — those labeled as types Ia (square-wave), Ib, II (parabolic) and IV — first occur in the unfoldings of codimension-three bifurcations, as was shown in [8] and as we will see here.

Remark 1.6. Ultimately a local classification of bursters, as we describe here, is limited by the extent to which universal unfoldings of dynamical singularities are understood. For example, in the classification of codimension-two bursters, the unfoldings of Hopf-steady state and Hopf-Hopf mode interactions are not yet completely understood in a rigorous fashion. We have only reported results here for the studies of the truncated normal forms and, hence, we can only say that our classification is complete to the extent that it is covered by the known theory. See section 1.3.4 and section 1.3.5 for more discussion. It seems likely, however, that these details will have little significant impact on our conclusions.

Remark 1.7. The singularity-based approach may be contrasted with that of Izhikevich [37]. Specifically, [37] has classified periodic bursters by the precise bifurcations that occur along the trajectory. Each distinct sequence of codimension-one bifurcations in the fast subsystem is considered as giving rise to a different type of burster. Also, the resultant sequence is labeled as a 'codimension-one' burster, e.g. a sequence is labeled as Hopf-Hopf when the active phase begins and ends with Hopf bifurcations. There is, therefore, a mixture of local and global in this classification scheme, whereas the singularity-based approach is purely local and intrinsic. In addition, it is not clear from the classification in [37] how 'likely' each of the given sequences is. In the singularity-based approach the possible sequences that occur in the unfolding of a given singularity can be seen directly. Moreover, since each of these sequences arises in an unfolding of a singularity, their intrinsic complexity is that of the associated singularity.

1.1.4 Generic Paths

Using transversality, loop space (the space of closed paths through the space of unfolding parameters $\mathbb{R}^k$) can be decomposed into connected components separated by a codimension-one variety. Again this decomposition into connected components is important only near the origin in loop space. We call a closed path $\mu : \mathbf{S}^1 \to \mathbb{R}^k$ *generic* if μ intersects $\mathcal{V}$ transversely.

Transversality implies that μ intersects $\mathcal{V}$ only in codimension-one components and crosses those components with nonzero speed. Therefore, transversality implies that any sufficiently small perturbation of a generic path is generic and that the two paths are path equivalent. Thus, the connected components of loop space mentioned above consist of paths that are all path equivalent. The variety separating these components consists of paths that are tangent to the variety $\mathcal{V}$ or that intersect $\mathcal{V}$ at points of codimension greater than one.

It seems quite difficult to classify all generic paths, that is, all components of generic paths in loop space. We sidestep this issue by mostly considering paths in the family

$$\mu(\theta) = A + \cos(\theta)B + \sin(\theta)C \tag{1.5}$$

where $A, B, C \in \mathbb{R}^k$ are vectors in parameter space. These paths are usually our candidates for paths supporting bursters. Note that this $3k$-dimensional subspace of loop space also divides naturally into components of generic paths.

This choice of paths in loop space can be motivated by thinking that there is a Hopf bifurcation in the slow equations that generates a family of periodic solutions in the slow variables. These periodic solutions then force the fast equation, since the slow variables are the parameters in the unfolding of the singularity in the fast equation. The family of paths obtained in this way is, to first order in a Fourier decomposition sense, the same as those in (1.5).

1.1.5 Organization of this chapter

In section 1.2 we analyze the standard Hopf singularity that gives rise to the unique codimension-one periodic burster. In section 1.3, we systematically study the known codimension-two singularities of vector fields and identify all of the codimension-two periodic bursters that they generate. Finally, section 1.4 is devoted to a particular codimension-three singularity in whose universal unfolding several codimension-three periodic bursters are found. We discuss the singularity in the fast system, the relevant paths through the unfolding of that singularity, and the associated time series for each burster type we consider.

1.2 The codimension-one burster

We begin the classification with bursters of codimension one. The generic codimension-one bifurcations of flows are saddle-node and Hopf bifurcations. However, paths in the unfolding space of a saddle-node bifurcation do not lead to bursting, since the fast system contains no stable states on one side of the bifurcation point. Thus, the sole codimension-one bifurcation of interest here is the Hopf bifurcation.

The nondegenerate Hopf bifurcation, also known as the Andronov-Hopf bifurcation [1, 32, 41], has the normal form (in polar coordinates)

$$\begin{aligned} r' &= r(\mu - r^2) + \mathcal{O}(r^4) \\ \theta' &= 1 + \mathcal{O}(r^2) \end{aligned} \tag{1.1}$$

where μ is a real number. Here, we have chosen the coefficient in front of the cubic term to be negative, since we are interested in the bifurcation to a stable limit cycle. It is known that the dynamics of (1.1) is topologically equivalent to that of the truncated normal form, the system (1.1) without the higher-order terms. Thus, we study the truncated normal form.

For each μ, the system (1.1) has an equilibrium at $r = 0$. It is a stable focus attracting all orbits at an exponential rate for each $\mu < 0$, whereas it is an unstable focus for any $\mu > 0$. The transition occurs precisely at the Hopf bifurcation point $\mu = 0$, where the origin is topologically a stable focus but orbits approach it at only an algebraic rate. For $\mu > 0$, there is also a unique limit cycle (of radius $\sqrt{\mu}$ in the truncated system (1.1)) that is asymptotically stable and attracts all nonzero initial conditions. In this case, the transition variety $\mathcal{V}$ is just the origin.

In order to study bursting, we make the unfolding parameter vary slowly along a closed loop:

$$\mu = C \sin(\epsilon t), \tag{1.2}$$

where $A = B = 0$ in (1.5) and $0 < \epsilon \ll 1$. This slow variation in the unfolding parameter μ causes the system to periodically cross the Hopf transition

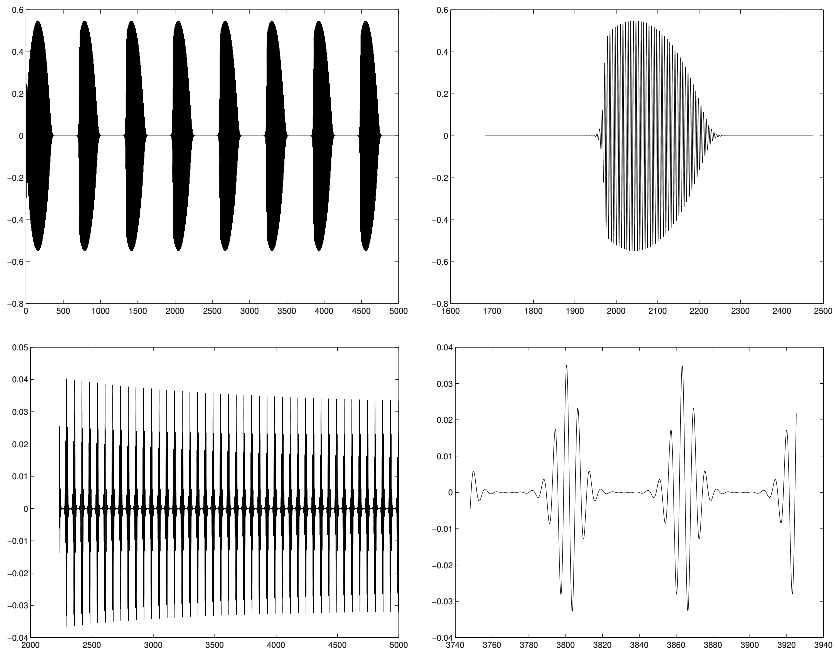

Figure 1.1. Time series of $r\cos\theta$ obtained from (1.1) and (1.2) with $C = 0.3$ for $\epsilon = 0.01$ (top; note the slow passage effect) and for $\epsilon = 0.1$ (bottom). The right panels show enlargements of a portion of the left panels so the spikes are visible. There are more spikes per burst event with $\epsilon = 0.01$ than with $\epsilon = 0.1$, since the frequency of the periodic orbit is $\mathcal{O}(1)$ in the fast time and, hence, the slower the slow variable changes, the more the fast variable oscillates.

variety. More generally, in terms of the paths $\mu(t) = A + B\cos(\epsilon t) + C\sin(\epsilon t)$ considered in (1.5), A, B, C space divides into three regions: one in which the path is always to the right of 0, one where it is always to the left of 0, and one where the path crosses the origin twice. The path given by (1.2) samples this last region and gives rise to bursting (in those cases where the slow passage effect permits it, see below). The other two regions are associated to paths that do not yield bursting.

There is an important additional phenomenon, namely slow passage through a Hopf bifurcation [42, 43], that arises in the system (1.1) with μ given by (1.2), for sufficiently small ϵ, as well as in other bifurcations in which the equilibria have eigenvalues with nonzero imaginary parts. For analytic vector fields, solutions will stay close to an unstable equilibrium point beyond the Hopf bifurcation value at which the equilibrium became unstable. Moreover, if there is a finite ($\mathcal{O}(1)$) buffer point, then the solutions will do so until the value of μ reaches the value of that buffer point and they will all leave a neighborhood of the unstable equilibrium point in an exponentially small interval about the buffer point. This delay in the effect of the bifurcation runs counter to one's intuition in that one would instead expect that solutions get repelled by the equilibrium as soon as it becomes unstable. Therefore, this slow passage effect plays a prominent role in determining the amplitude profile of the burster. See figure 1.1 for the manifestation in the analytic Hopf burster, and we refer the reader to some of the by-now large literature on slow passage; see [4, 7, 14, 21, 34, 42, 43, 61, 62]. For completeness, it is also worth recalling here that noise will destroy the slow passage effect; see [4, 42, 43].

1.3 Codimension-two bursters

The next simplest bursting types are those of codimension two. In this section, we analyze each of the generic codimension-two local singularities in the fast system to classify codimension-two bursters. These are

(i) the cusp point,
(ii) the degenerate Hopf bifurcation point,
(iii) the Takens-Bogdanov bifurcation point,
(iv) the Hopf-steady state bifurcation point, and
(v) the Hopf-Hopf bifurcation point.

These systems have two-dimensional unfolding spaces and, within the framework of section 1.1, we take the unfolding parameter μ to be of the form

$$\begin{aligned} \mu_1 &= B_1 \cos(\epsilon t) + A_1 \\ \mu_2 &= C_2 \sin(\epsilon t) + A_2. \end{aligned} \tag{1.1}$$

1.3.1 The cusp

The cusp is a saddle-node bifurcation in which there is a degeneracy in the quadratic terms. This bifurcation involves the transition from one steady-state to three. The universal unfolding is given by:

$$\dot{x} = -x^3 + \mu_1 x + \mu_2 + \mathcal{O}(x^4). \tag{1.2}$$

Here also, the dynamics of the full normal form (1.2) is topologically equivalent to that of the truncated system, i.e., (1.2) without the higher order $\mathcal{O}(x^4)$ terms. Hence, the bifurcation diagrams are qualitatively the same, so that one only needs to study the truncated system; see [26, chapter III.12(c)] or [39, chapter 8.2].

Following the framework of section 1.1, we find the transition variety for the cusp singularity. In (μ_1, μ_2, x)-space, the edges of the cusp surface

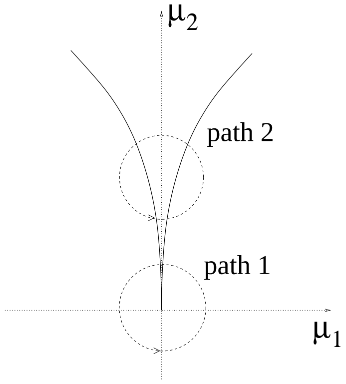

Figure 1.2. The projection of the cusp surface $-x^3+\mu_1 x+\mu_2=0$ onto the plane of the unfolding parameters. The cusp curves are given by $(\mu_1/3)^3=(\mu_2/2)^2$. Paths 1 and 2 lead to the two different types of bursting. The corresponding time series are given in figure 1.3.

are given by $(\mu_1,\mu_2)=(3x^2,-2x^3)$. Hence, the cusp curves, which are the projections of these edges onto the μ_1,μ_2 plane, are given implicitly by

$$\left(\frac{\mu_1}{3}\right)^3=\left(\frac{\mu_2}{2}\right)^2. \tag{1.3}$$

See figure 1.2. For points (μ_1,μ_2) inside the cusp curve, the cubic has three distinct real roots, whereas outside of it, there is only one real root. The cusp curves correspond to bifurcations along which two equilibria exist (one of which is a saddle-node point).

Among the closed paths of the type considered in section 1.1, there are two distinct types that give rise to periodic bursters. These are illustrated in figure 1.2, and the corresponding time series with the unfolding parameters μ_1,μ_2 varying as in (1.1) are shown in figure 1.3. In figure 1.3(left) μ_1,μ_2 vary slowly around a circle centered at the origin (path 1 in figure 1.2). Along part of this circle, the system is in the regime with only one equilibrium, while for parameter values along the remainder of this circle, the system is in the three equilibrium regime. Hence, the time series in the left frame exhibits only one rapid jump (down) each period. By contrast, the time series in figure 1.3(right) exhibits two rapid jumps (one up and one down) each period. This time series was generated instead by choosing a circle in parameter space that crosses each branch of the cusp (transition) variety twice, once in each direction; see path 2 in figure 1.2.

In the remainder of this subsection, we show how the method of section 1.1 also yields computable conditions on the parameters B_1, C_2, A_1 and A_2 under which the circular paths are tangent to the cusp curve. For sim-

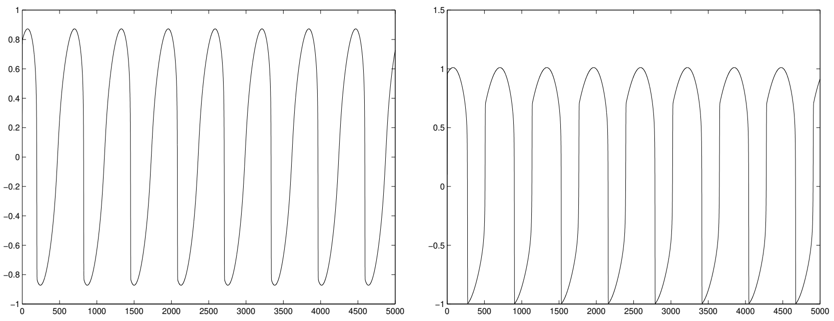

Figure 1.3. The time series $x(t)$ of the solutions of (1.2) with the unfolding parameters given by (1.1) with $B_1 = C_2 = 0.5$ and $(A_1, A_2) = (0, 0)$ (left panel) and $B_1 = C_2 = 0.3$ and $(A_1, A_2) = (0, 0.6)$ (right panel). These formulae correspond to paths 1 and 2, respectively, in figure 1.2. In both cases $\epsilon = 0.01$.

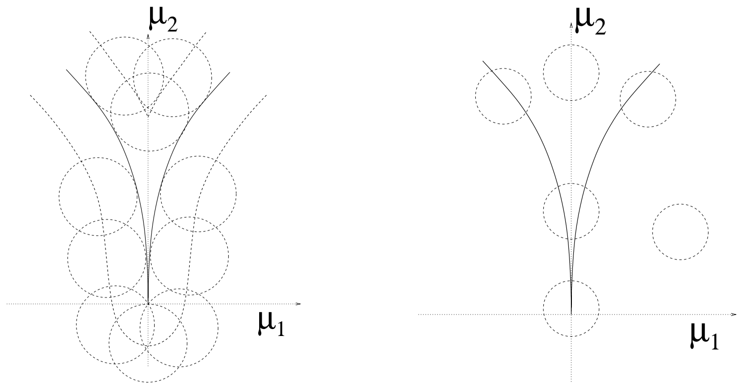

Figure 1.4. Left panel: sketch of the family of circles that are tangent to the cusp curves and of the locus of points at which these circles are centered, as computed in section 1.3.1. Right panel: Members of the six components in the space of circular paths which are separated by the families of paths depicted on the left.

plicity of calculation throughout, we transform the unfolding parameters to $\nu_1 = \frac{-\mu_2}{2}$, and $\nu_2 = \frac{\mu_1}{3}$. Hence, the cusp curves are given by

$$\nu_1^2 = \nu_2^3. \tag{1.4}$$

We let $B_1 = C_2 = R$ and rewrite the paths in the more convenient form

$$(\nu_1, \nu_2) = (R\cos(\tau) + A_1, R\sin(\tau) + A_2). \tag{1.5}$$

Parametrically, the tangency condition is then $2\nu_1\nu_1' - 3\nu_2^2\nu_2' = 0$, subject of course also to the condition that (1.4) holds. Solving (1.5) for the trigonometric functions and recalling that $R > 0$, the tangency condition becomes

$$2\nu_1(\nu_2 - A_2) + 3\nu_2^2(\nu_1 - A_1) = 0. \tag{1.6}$$

Finally, the locus of points at which the circles must be centered so that they are tangent to the cusp transition variety may now be found parametrically. Fixing R and solving (1.6) for ν_1 in terms of ν_2 and then by plugging this into (1.4), one obtains a quartic equation for ν_2 whose coefficients depend on A_1 and A_2. Analysis of this quartic then leads to the desired locus of (A_1, A_2) values; see figure 1.4.

Remark 1.8. The behavior studied in this subsection would not traditionally be considered to be bursting, since the active phase involves only a stable equilibrium and not a periodic state.

1.3.2 Degenerate Hopf bifurcation

The next codimension-two singularity also arises when there is a degeneracy in a codimension-one point. In particular, we focus on the codimension-two degenerate Hopf bifurcation to a stable limit cycle; see [2, 6, 63]. The full normal form is:

$$\begin{aligned} r' &= (\mu_1 + \mu_2 r^2 - r^4)r + \mathcal{O}(r^6) \\ \theta' &= 1 + \mathcal{O}(r^2). \end{aligned} \tag{1.7}$$

The normal form of (1.7) is again topologically equivalent to that of the truncated normal form, i.e., (1.7) without the higher-order correction terms. Also, the remaining codimension-two degenerate Hopf bifurcations not considered here has a plus sign of the quintic term, and a similar analysis can be carried out for it.

Hopf bifurcations occur when $\mu_1 = 0$, and saddle-node bifurcations of periodic orbits occur along the curve $\mu_1 = -\frac{\mu_2^2}{4}$; see figure 1.5.

To generate the associated codimension-two burster, we let the unfolding parameters evolve as in (1.1). Examples of the four paths that lead to the four different periodic bursting types are shown in figure 1.5. Path 1 leads to nondegenerate Hopf bursting studied in section 1.2. Paths 2 and 3 also create bursting types that involve transitions between a stable equilibrium and a stable limit cycle. However, these bursters are distinguished by whether the transition between the states is a smooth one (a Hopf bifurcation) or a jump transition (caused either by a subcritical Hopf bifurcation or by a saddle-node of limit cycles); see figure 1.6 for the corresponding time series and also [36].

The bursting obtained from path 4 is a type III burster; see figure 1.7. Thus, type III bursters are of codimension two by definition 1.5. It should

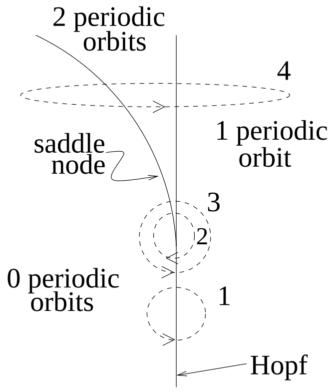

Figure 1.5. The (μ_1, μ_2) plane for degenerate Hopf bifurcation. There are three regions: with zero, one, or two periodic orbits, respectively, and in each region there is also an equilibrium at $r = 0$. Paths 1-4 lead to different bursting types. Path 1 leads to Hopf bursting; see section 1.2. For bursting along paths 2-4; see figure 1.6 and figure 1.7. Note that the discussion immediately after definition 1.4 implies that changing the direction along paths 1 and 4 does not lead to new bursting types.

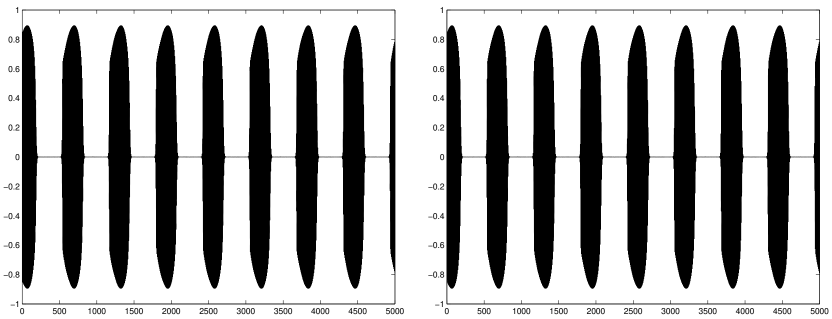

Figure 1.6. Time series corresponding to paths 2 and 3 in figure 1.5. For path 2 (left) the subcritical Hopf bifurcation causes a jump to a stable limit cycle followed by a Hopf bifurcation; for path 3 (right) there is a Hopf bifurcation to a limit cycle followed by a saddle-node of limit cycles. For both paths $B_1 = C_2 = 0.5$ and $(A_1, A_2) = (0, 0)$. Furthermore, $\epsilon = -0.01$ for path 2 and $\epsilon = 0.01$ for path 3, so the two paths are traversed in opposite directions. Both frames show the slow passage effect at the start of the active phases.

be noted that the states of the fast system and their bifurcations are the same as those in [8]. Due to the form of the equations in [8] the total

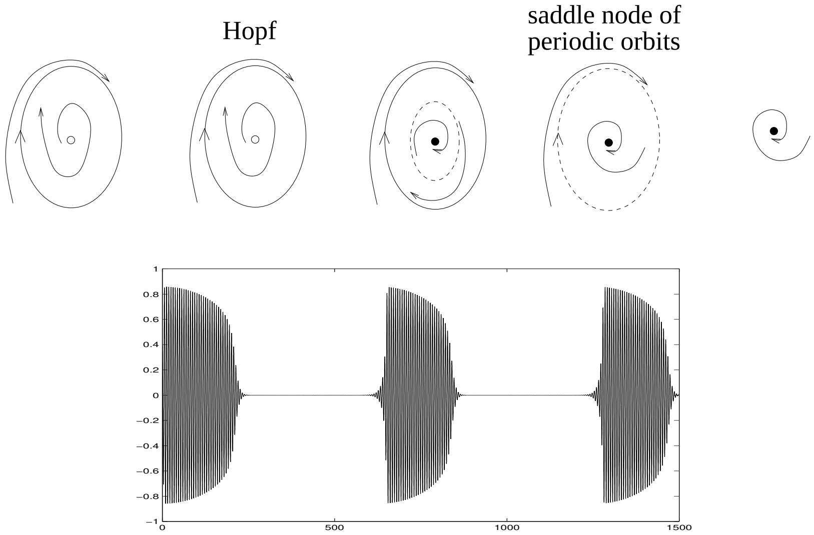

Figure 1.7. A schematic representation of type III bursting (top) and the time series (bottom) of $r\cos\theta$ generated by (1.7) and (1.1) with $B_1 = C_2 = 0.15$, $A_1 = -0.05$, $A_2 = 0.6$ and $\epsilon = 0.01$ (corresponding to path 4 in figure 1.5). The stable and unstable periodic orbits collide in a saddle-node of periodic orbits, causing the system to return to the quiescent state. The slow passage effect is manifested at the beginning of each active phase.

number of bifurcations that the fast system undergoes during one period of the slow system is greater than in the present case. However, the sequence of states visited by the fast system and their bifurcations are the same in both examples. Therefore according to definition 1.2 we may say that both systems exhibit type III bursting.

We also remark that the time series of this type III burster may seem slightly unfamiliar, since the radius of the limit cycle is changing, whereas in the standard case the radius is almost constant. A naive reckoning leads to the same conclusion, since one needs two parameters to arrange for the two essential topological characteristics of type III bursters to occur, namely that the active phase begins in a subcritical Hopf bifurcation and that the burst terminates in a saddle-node of periodic orbits. Of course, type III bursters can also be found in the unfoldings of higher codimension singularities; see for example [8, Section 4] where it is shown that type III bursting occurs in the unfolding of the degenerate Takens-Bogdanov bifurcation studied in [22].

Remark 1.9. The bursters corresponding to paths 2, 3 and 4 are the first bistable bursters that we have encountered.

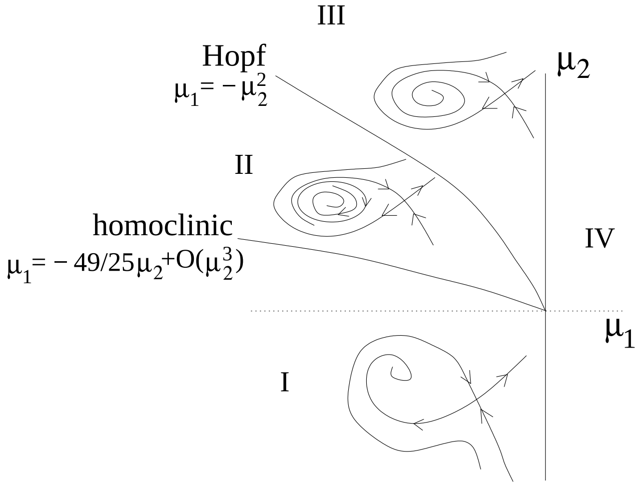

Figure 1.8. Bifurcation diagram in the unfolding space of a Takens-Bogdanov point.

Remark 1.10. Here, we have studied singly-degenerate Hopf bifurcations, i.e., the codimension-two case. Hopf bifurcations with higher-order degeneracies and/or symmetries also occur in the full normal form, in which case the resulting bursting type is of codimension three or higher; see [63].

1.3.3 Takens-Bogdanov bifurcation

The Takens-Bogdanov bifurcation involves a double zero eigenvalue, and the universal unfolding has the form:

$$\begin{aligned} x' &= y \\ y' &= \mu_1 + \mu_2 y + a x^2 + b x y + \mathcal{O}(3) \end{aligned} \tag{1.8}$$

where μ_1 and μ_2 are the unfolding parameters, $a = 1$, $b = \pm 1$, and $\mathcal{O}(3)$ indicates third-order terms in x and y. Complete studies of this unfolding were first presented in [9, 10] and [64]. Moreover, as in the previous sections, here also the bifurcation diagrams of the truncated normal form are not qualitatively changed by the addition of the higher order terms, so that it suffices to study the truncated system.

Figure 1.8 schematically depicts the dynamics in the different parameter regions of (1.8) when $b = 1$. The curve $\mu_1 = -\mu_2^2$ separating regions II and III is a locus of Hopf bifurcations, while the curve $\mu_1 = -(49/25)\mu_2^2 + O(\mu_2^3)$ separating regions I and II is a locus of homoclinic bifurcations; see [20, chapter 4.1], [30, chapter 7.3] or [39, chapter 8.4]. The case $b = -1$ is similar.

Although the unfolding of this bifurcation is the most complicated we have considered so far, it does not lead to any new bursting types. The system does not have any stable attracting states when the unfolding parameters are in regions III and IV. Hence, only paths that remain in regions I and II are of interest. More specifically, only those paths crossing the locus of homoclinic bifurcations between regions I and II need to be considered. However, no such path leads to bursting, since the origin is a stable equilibrium on both sides of the homoclinic bifurcation. Finally, if the flow of the fast system is reversed in time (i.e., the arrows in figure 1.8 point in the opposite directions), then there will be a stable limit cycle in region II and a stable point in region III and no stable states in regions I and IV. Therefore, this case only leads to the codimension-one bursting already considered in section 1.2, since regions II and III are separated by a locus of nondegenerate Hopf bifurcation points.

1.3.4 Hopf-steady state bifurcation

In order to observe a Hopf-steady state bifurcation, the fast system must be of dimension three or higher. The normal form of this bifurcation is

$$\begin{aligned} r' &= \mu_1 r + arz + rz^2 + \mathcal{O}(|r,z|^4) \\ z' &= \mu_2 + br^2 - z^2 + \mathcal{O}(|r,z|^4) \\ \theta' &= \omega + c_1 z + \mathcal{O}(|r,z|^2) \end{aligned} \tag{1.9}$$

where either $b = 1$ or $b = -1$; see [20, chapter 4.6] or [39, chapter 8.5]. We focus here exclusively on the truncated normal form, which is (1.9) without the higher order terms and with $c_1 = 0$. This truncated normal form is exact when there are certain symmetries in the vector field [20, 39]. However, for general systems, the higher order terms *do* qualitatively alter the bifurcation diagram of the truncated system, leading to various global phenomena and chaotic states. Therefore, in this case (and in that of the Hopf-Hopf bifurcation considered in the next section) the truncated and full normal forms are not topologically equivalent, in contrast to the bifurcations analyzed in sections 1.3.1 to 1.3.3. These two singularities were studied in [24], and the proof of uniqueness of the limit cycle was first given in [71, 72].

The main new bursting observed here involves a stable equilibrium bifurcating into a stable limit cycle and then into a stable two-torus, along with the attendant quasi-periodic spiking observed during the active phase. This occurs for example in the time reversed (1.9) with $a = 0.5$, $b = -1$, $c_1 = 0$, $\omega = 0.005$ and the path:

$$(\mu_1, \mu_2) = 0.03(\cos(g(\epsilon t)), \sin(g(\epsilon t))) \quad \text{where} \quad g(\epsilon t) = 0.865 + 0.815\cos(\epsilon t). \tag{1.10}$$

See figure 1.9 and figure 1.10.

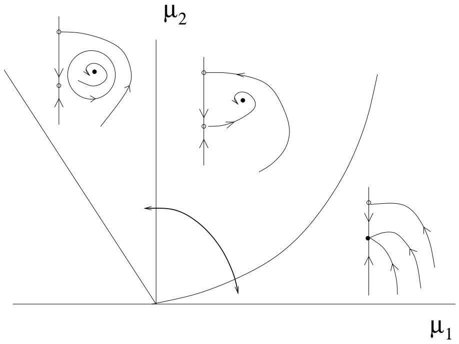

Figure 1.9. Sketch of the path (1.10) for the system (1.9) with $a = 0.5$, $b = -1$, $c_1 = 0$, and time reversed. The corresponding time series is shown in figure 1.10.

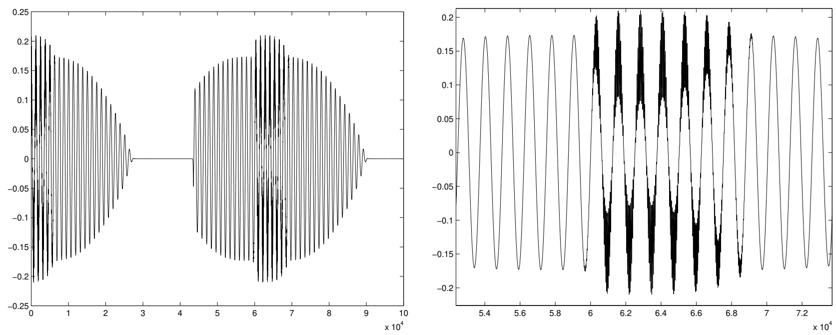

Figure 1.10. Left panel: Time series of the variable $x = r\cos\theta$ generated by (1.9) with the path (1.10) shown in figure 1.9 and with $\epsilon = 0.0001$. The stable equilibrium at $r = 0$ undergoes a Hopf bifurcation to a stable limit cycle (with $r(t)$ slowly growing), which in turn bifurcates into a stable two-torus (with $r(t)$ oscillating rapidly) via a Neimark-Sacker bifurcation. The delayed passage effect is clearly visible in both bifurcations. Right panel: Enlargement of the transitions from periodic to quasi-periodic to periodic solutions.

Bursting to a two-torus occurs more generally when $b = -1$, $a > 0$ and time is reversed in (1.9), i.e., when one is in what is traditionally labeled as case III (with time reversed) in the analysis of the Hopf-steady state bifurcation. In this case, there are both a Hopf bifurcation curve and a Neimark-Sacker bifurcation curve (bifurcation of a limit cycle into a two-torus); see [20].

The other cases, corresponding to $b = 1$ and $a > 0$, $b = 1$ and $a < 0$, and $b = -1$ and $a < 0$, respectively, are analyzed in the appendix. However, a systematic search reveals that there are no other new types of bursting.

1.3.5 Nonresonant Hopf-Hopf bifurcation

Hopf-Hopf bifurcations arise when there is a singularity that has a pair of nonresonant, purely imaginary eigenvalues. The fast system must be of dimension four or higher. The normal form [20] is:

$$\begin{aligned}
r_1' &= r_1(\epsilon_1 + p_1 r_1^2 + p_2 r_2^2 + q_1 r_1^4 + q_2 r_1^2 r_2^2 + q_3 r_2^4) + \mathcal{O}(|r|^6) \\
r_2' &= r_2(\epsilon_2 + p_3 r_1^2 + p_4 r_2^2 + q_4 r_1^4 + q_5 r_1^2 r_2^2 + q_6 r_2^4) + \mathcal{O}(|r|^6) \\
\theta_1' &= \omega_1 + \mathcal{O}(|r|^2) \\
\theta_2' &= \omega_2 + \mathcal{O}(|r|^2).
\end{aligned} \tag{1.11}$$

As in section 1.3.4, we consider the truncated normal form here, and the same comment about the impact of the higher order terms also applies here.

Since θ_1' and θ_2' are constant to second order, it is sufficient to consider the planar system (r_1, r_2). A change of coordinates, together with a nondegeneracy condition, takes the first two equations of system (1.11) up to sixth order to

$$\begin{aligned}
\sigma x' &= x(\mu_1 + \eta x - y + q_1 x^2 + q_2 xy + q_3 y^2) \\
\sigma y' &= y\left(\mu_2 - \tfrac{\alpha+1}{\beta}\eta x + \tfrac{\alpha}{\beta+1} y + q_4 x^2 + q_5 xy + q_6 y^2\right)
\end{aligned} \tag{1.12}$$

where $\sigma, \eta = \pm 1$, $x \geq 0, y \geq 0$, and μ_1 and μ_2 are the unfolding parameters. The sign of σ allows us to change the direction of time in the normal form. The study of this system can be reduced to 16 cases, some of which are equivalent. We refer the reader to [20, chapter 4.7] for details.

We have carried out a full analysis of these 16 cases, and many of the bursters occurring in its unfolding are of types that have already been described. Therefore, rather than presenting a full description of all the unfoldings, we will concentrate on the unfoldings that lead to new bursting types. We also emphasize that the results below are stated in terms of the planar system (1.12), unless otherwise stated.

Case 1. $\eta = -1$, $\alpha > 0$, $\beta > \alpha$, and $\sigma = -1$ (Case a_- with time reversed in [20]). Here, we find a new periodic bursting type that involves a stable three-torus. In particular, the following sequence of bifurcations can be observed for the path

$$\mu_1(\epsilon t) = 0.3 \quad \text{and} \quad \mu_2(\epsilon t) = -0.12 + 0.13\sin(\epsilon t) \tag{1.13}$$

(see figure 1.11) with $\epsilon = 0.003$ $\alpha = 1$ and $\beta = 2$, as well as for general paths like it in the μ_1, μ_2 unfolding space. The corresponding time series is shown in figure 1.12. A stable state appears from the origin in a saddle-node bifurcation. This new stable state on the y-axis loses its stability, giving birth to another stable state in the region $x > 0, y > 0$, as the

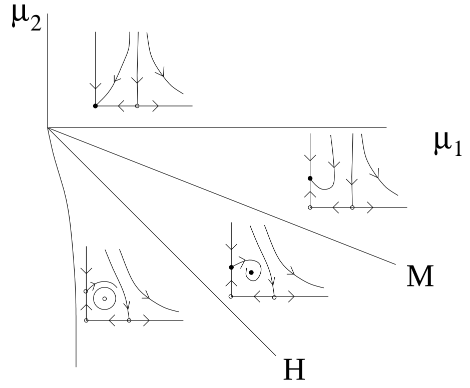

Figure 1.11. Part of the parameter space for case 1 of (1.12).

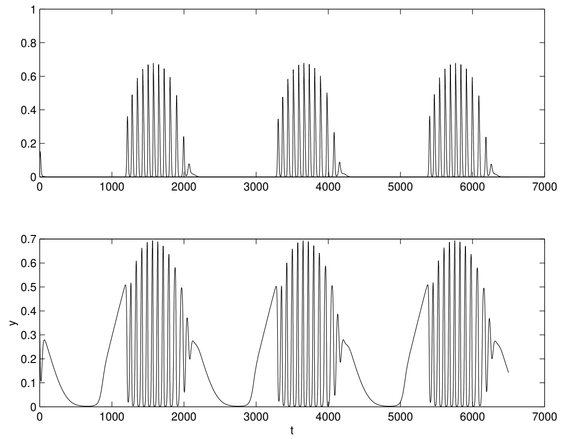

Figure 1.12. Time series of $x = r_1 \cos\theta_1$ (top) and of $y = r_2 \cos\theta_2$ (bottom) for Case 1 of the Hopf-Hopf bifurcation, generated by (1.12) with $q_1 = 1$ and $q_2, \ldots, q_6 = 0$. The slow passage effect causes the delayed (and abrupt) onset of the oscillation.

path crosses the curve M. This last stable state loses its stability via a supercritical Hopf bifurcation (on the curve marked H in figure 1.11). As the second half of the path is traversed, these bifurcations occur in reverse order. Note that, in the full system (1.11), this sequence of bifurcations becomes: a stable equilibrium at the origin undergoes a Hopf bifurcation to a stable limit cycle, which undergoes a Neimark-Sacker bifurcation to a stable two-torus, which finally bifurcates to a stable three-torus (with the appropriate slow passage effect at each stage), and then back again.

Since there is only one stable state for each of the parameter regions, this bursting type is not bistable.[1]

Case 2. $\eta = -1$, $\beta > 0$, $\beta < -\alpha - 1$, and $\sigma = 1$ (Cases d_- and h_- in [20]). For a range of parameter values, there is a bistable regime with stable states on the x- and y-axes. At each of the borders of this regime a saddle from the region $x > 0, y > 0$ collides with one of these states, leading in both cases to an exchange of stability. Therefore, a path traversing this region in parameter space will lead to the fast system jumping between the two stable states (limit cycles). In other words, in the full system, one pair of variables will be active while the other pair is quiescent, and at each bifurcation the roles of the two pairs are reversed.

Case 3. $\eta = +1$, $\alpha > 0$, $\beta > \alpha$, and $\sigma = -1$ (Case a_+ with time reversed in [20]). This case is similar to the preceding one, except that there is no bistability. There is a region of parameter space in which the origin is stable, and the origin gives birth to stable states on the x and y axes, respectively, at the boundaries of this region. A path traversing this region and part of the adjacent regions will lead to the stable state approaching these three stable states in turn. In the full system this will lead to bursting similar to the one discussed in the previous case. The main difference is that, while there are abrupt jumps between the two oscillating states in the last examples, in this case the amplitudes decay to the point where both pairs of variables are quiescent before the cycle starts again.

Case 4. $\eta = +1$, $\beta > 0$, $\beta < -\alpha - 1$, and $\sigma = 1$ (Case d_+ in [20]). In this case, a sequence of bifurcations starting from a stable state at the origin leads to the appearance of a stable limit cycle, as in the first case. Therefore, an appropriate path in the parameter space will lead to the same type of bursting. However, at the parameter values at which the limit cycle exists, the origin is also stable leading to the possibility of bursting from the quiescent state to a 3-torus in the full system. Moreover, since the size of the limit cycle becomes greater than $\mathcal{O}(\epsilon_1, \epsilon_2)$ before it loses stability, the normal form cannot give a full picture of this case.

Remark 1.11. These bursting types also occur at other parameter values. They represent all the new bursting types in the case of two purely imaginary eigenvalues without resonances. We refer the reader to [35], for example, for the normal form in the case of the 1:1 resonant Hopf-Hopf bifurcation.

[1] Although it is of codimension two, this bursting type is not listed in the classification of [37].

1.4 Codimension-three bursters

Whereas in the previous sections we were able to give an exhaustive treatment of all of the known generic codimension-one and -two bifurcations, our goal here is limited to showing that the traditional bursters of types Ia, II and IV can be found explicitly using the framework of section 1.1 in the unfolding of a particular codimension-three singularity. This was already noted in [8].

Our goal must necessarily be limited since the unfoldings of only very few codimension-three singularities are known. Those unfoldings that are known are for codimension-three singularities of generic three-parameter planar vector fields, namely the swallow-tail bifurcation, the Takens-Hopf bifurcation, and the degenerate Takens-Bogdanov bifurcations with either a double or a triple equilibrium; see the bibliographical notes in [39, chapter 8]. In contrast, the study of codimension-three singularities in higher-dimensional fast systems is far from complete.

1.4.1 Type Ia bursting

Type Ia bursters, also known as square wave bursters, are characterized by monotonically decreasing spike frequency, i.e., increasing inter-spike intervals. The fast system is typically two-dimensional and bistable, and the variation of a single slow variable causes the fast systems to visit both attractors in a time-periodic manner; see figure 1.15. The burst (or active phase) begins at a saddle-node of equilibria in the fast system, where the trajectory jumps from a branch of stable equilibria to a branch of stable periodic orbits. The frequency of these periodic orbits decreases during the active phase until the family of periodic orbits disappears in a saddle-loop connection (homoclinic bifurcation). This saddle-loop connection, in turn, marks the end of the active phase, since near it the trajectory must jump back to the original branch of stable equilibria. Geometric singular perturbation theory treatments of type Ia bursters are given in [56, 66].

Thus, the bursting behavior is due to two dynamic bifurcations in the system: a saddle-node and the breaking of a homoclinic connection. From the classifications of codimension-one and -two bursters given in the previous sections, we see that these two bifurcations were not encountered in the unfoldings studied there. Hence, we know that the minimum codimension of a type Ia burster must be at least three.

The codimension turns out to be exactly three, as we now show. In particular, we study a codimension-three degenerate Takens-Bogdanov point and use its truncated normal form as the fast system of our burster to show explicitly how type Ia bursting occurs in the framework of section 1.1:

$$\begin{aligned} x_1' &= x_2 \\ x_2' &= -x_1^3 + \mu_2 x_1 + \mu_1 + x_2(\nu + 3x_1 + x_1^2). \end{aligned} \tag{1.14}$$

We focus here on those features of (1.14) that are of interest to us and, hence, do not consider the entire universal unfolding, which is quite complicated (see [22], though note that we have taken a slightly different form). Our principal goal is to locate a point at which both a homoclinic (saddle-loop) bifurcation and a saddle-node bifurcation occur. We label such a point HSN. Moreover, the procedure we use here to find the HSN point can be implemented numerically, so that this example also illustrates the computational advantage of the singularity-based approach.

The fixed points of (1.14) are given by

$$x_1^3 = \mu_2 x_1 + \mu_1, \qquad x_2 = 0 \tag{1.15}$$

and the Jacobian of the vector field at $(x_1, 0)$ equals

$$DF(x_1, 0) = \begin{pmatrix} 0 & 1 \\ -3x_1^2 + \mu_2 & \nu + 3x_1 + x_1^2 \end{pmatrix}. \tag{1.16}$$

The condition that a fixed point is also a saddle-node bifurcation point is then that the bottom left entry of (1.16) vanishes, so that for $\mu_2 > 0$, we find $x_1^2 = \mu_2/3$.

Now, to further simplify our calculations, we choose $\mu_2 = 1/3$ and illustrate the results below in the $\mu_1 - \nu$ parameter plane

$$P = \{(\mu_1, \mu_2, \nu) \in \mathbb{R}^3 : \mu_2 = 1/3\}.$$

Computations for other values of μ_2 proceed in the same fashion. This simplifying choice implies that the fixed points $(x_1 = \pm 1/3, x_2 = 0)$ are saddle-node points, which due to condition (1.15) exist when $\mu_1 = \mp 2/27$. Hence, on P, the vertical lines $\mu_1 = \mp 2/27$ are labeled as saddle-node lines. Furthermore, there is a single point on each of these saddle-node lines at which the fixed point degenerates into a Takens-Bogdanov point. These occur precisely where the bottom right entry of the Jacobian also vanishes, i.e., at $\nu = -10/9$ and at $\nu = 8/9$, respectively, for $\mu_1 = \mp 2/27$ and $x_1 = \pm 1/3$.

In the remainder of this analysis, we focus only on the first Takens-Bogdanov point at $(\mu_1, \nu) = (-2/27, -10/9)$ on P and on the bifurcation curves emanating from it. A similar analysis may be performed for the second Takens-Bogdanov point. There exists a Hopf bifurcation curve emanating from the first Takens-Bogdanov point, and on P this curve reaches the opposite saddle-node line ($\mu_1 = 2/27$) at the point with $\nu = -22/9$. This may be seen by observing that when $\mu_1 = 2/27$, the second fixed point (in addition to one with $x_1 = -1/3$) of the system (1.14) is at $(x_1 = 2/3, x_2 = 0)$ and that the condition for this second point to be a Hopf bifurcation point is that the bottom right entry in the Jacobian vanishes there, so that we find $\nu = -22/9$.

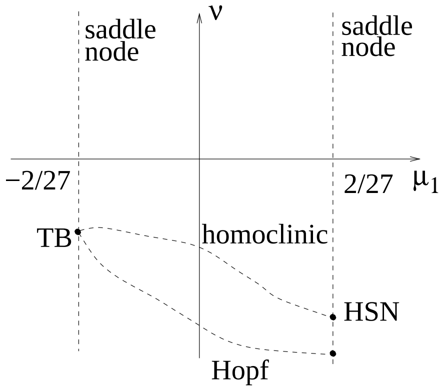

Figure 1.13. Part of the bifurcation diagram of (1.14) on P. The codimension-two point at which both a homoclinic and a saddle-node bifurcation occur is labeled HSN.

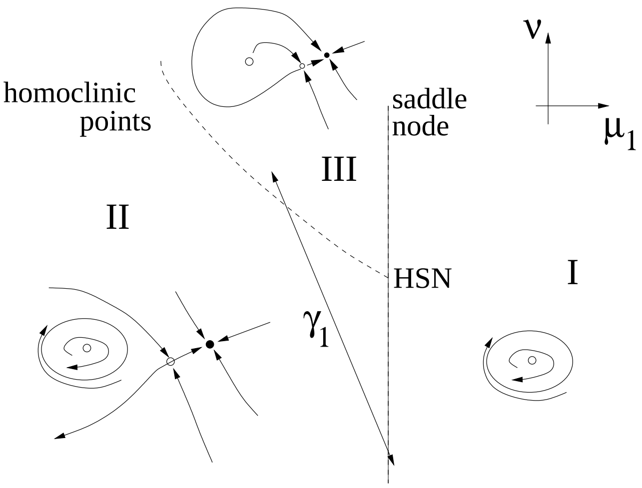

Figure 1.14. The path γ_1 in the universal unfolding of (1.14) leading to type Ia bursting.

Finally, it can be checked numerically that the locus of homoclinic bifurcations emanating from the first Takens-Bogdanov point intersects the opposite vertical line $\mu_1 = 2/27$ on P at approximately $\nu = -2.083$. Hence, the desired HSN point is located at $(2/27, -2.083)$; see figure 1.13.

We now choose a path that intersects both a surface of homoclinic bifurcations and a surface of saddle-node bifurcations. In particular, the path we choose in P is as shown in figure 1.14, which is a magnification of

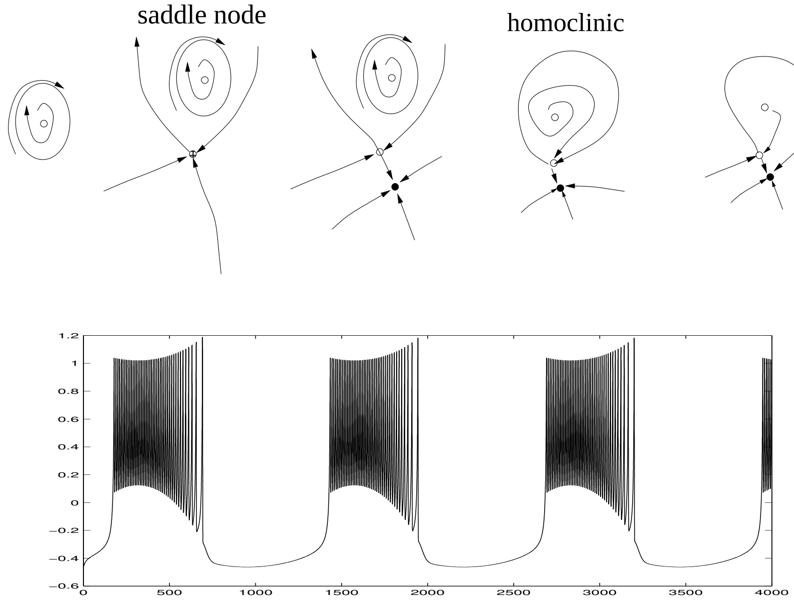

Figure 1.15. A schematic representation of type Ia bursting (top) and the time series generated by (1.14) with (1.17) and $\epsilon = 0.005$ and $\mu_2 = 1/3$ (bottom). This corresponds to the path γ_1 through the unfolding space shown in figure 1.14. In the top sequence of phase portraits, the lower fixed point disappears in a saddle-node bifurcation, and the system jumps to the periodic orbit. After the periodic orbit disappears via a homoclinic connection, the system returns to the fixed point, and the cycle repeats. The filled circles represent stable fixed points.

figure 1.13 around the point HSN

$$(\mu_1(t), \nu(t)) = (0.07 + 0.015\sin(\epsilon t), -2.1 - 0.15\sin(\epsilon t)). \qquad (1.17)$$

The sequence of bifurcations corresponds exactly to the sequence of bifurcations in type Ia bursting.

Remark 1.12. We refer the reader to [58] for a detailed analysis of the saddle-node separatrix-loop bifurcation.

Remark 1.13. Type Ib bursters are similar to type Ia bursters in that the two-dimensional fast system is also bistable and the spike frequency decreases during the active phase until a homoclinic bifurcation is reached. However, type Ib bursting differs in that the stable periodic orbits encircle three equilibria of the fast system, rather than just one, which results in the spikes being more widely spaced and in there being an undershoot after each spike independently of the chosen projection. Moreover, there need not be a spike plateau. Three is also the minimum codimension of the singularity in the fast system that is needed to support type Ib bursting, and hence type Ib periodic bursters are also of codimension three according to definition 1.5.

1.4.2 Type II bursting

Type II bursting is characterized by a parabolic plot of time-versus-spike frequency in which the frequency is small at the beginning and end of the active phase and larger in the middle. Hence, this phenomenon is also known as parabolic bursting. The two-dimensional fast system possesses an invariant circle; and, as a result of time-periodic changes in a two-dimensional slow variable, fixed points are created and destroyed in saddle-node bifurcations on this circle. In particular, during the quiescent phase, there are two equilibria on the circle, and the system is near the stable equilibrium. The disappearance of these equilibria in a saddle-node triggers the onset of the active phase, since then orbits on the invariant circle are free to travel around the circle periodically in time, producing spikes. Moreover, the frequency increases as the system moves further from the bifurcation point until it reaches a maximum, which corresponds to the vertex of the parabola. During the remainder of the active phase, the frequency decreases, and the active phase ends when there is again a saddle-node bifurcation in which the two equilibria re-emerge on the invariant circle. Examples are given in [5, 23, 55, 60, 68].

The saddle-node bifurcation on an invariant circle (SNIC) is a global bifurcation. In the classification of codimension-one and -two bursters given in the previous sections, we did not encounter it in the unfoldings of any of the local singularities. In fact, to observe a SNIC in an unfolding of a local bifurcation point, one needs to look at a singularity of codimension three or higher. We will establish, in this section, that type II bursting is of codimension three, according to definition 1.5. We do this by studying the same explicit example (1.14) of a codimension-three singularity. In the unfolding space of this singularity one can also construct paths leading to type II bursting. Such a degenerate point has previously also been used to generate type II bursting in [8].

Examination of figure 1.14 shows that a SNIC bifurcation occurs on the line separating regions I and III above the point HSN. Therefore, a path γ crossing the surface of saddle-node bifurcations from region I into region III will lead to type II bursting. The paths

$$(\mu_2(t), \nu(t)) = (0.333 + 0.02\sin(\epsilon t), -2.05)$$
$$(\mu_2(t), \nu(t)) = (0.333 + 0.02\sin(\epsilon t), -2.05 + 0.002\cos(\epsilon t))$$

with $\epsilon = 0.003$ lead to type II bursting; see figure 1.16.

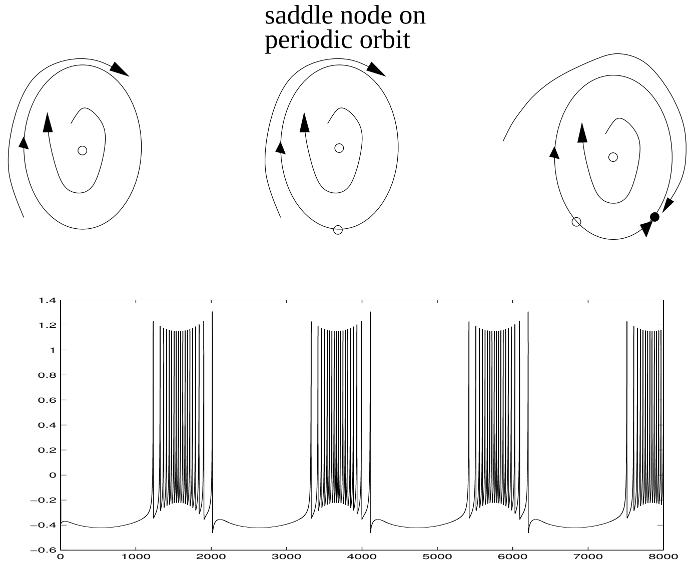

Figure 1.16. A schematic representation of type II bursting (top) and the time series generated by (1.14) and (1.18) with $\epsilon = 0.003$ (bottom). The oscillation stops due to a saddle-node bifurcation on the periodic orbit. The corresponding bifurcation diagram is given in section 1.4.2.

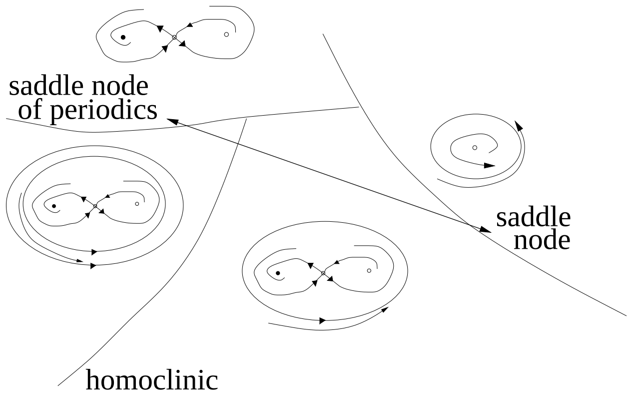

Figure 1.17. A path γ in the unfolding of (1.14) leading to type IV bursting.

1.4.3 Type IV bursting

Although type IV bursting is similar to type III bursting (encountered in section 1.3.2) since the bursting phase is terminated by a saddle-node of periodic orbits, it is of higher complexity than the latter. The reason for this is that, at the end of the quiescent phase, the stable fixed point loses stability through a saddle-node bifurcation rather than a Hopf bifurcation as in the case of type III bursting; see figure 1.17. This situation does not occur in any of the unfoldings of codimension-one or -two singularities, but it does occur in the unfolding of a degenerate Takens-Bogdanov point of focus type, as is shown in [8]. Therefore, this bursting type has codimension three.

One can carry out an analysis of the truncated normal form as in section 1.4.1 to find a path in parameter space that leads to this type of bursting. The details of the calculations are very similar to those given there.

Acknowledgements

We thank Ian Stewart for many helpful discussions about the local structure of bursters. The research of MG was supported in part by NSF Grant DMS-0071735 and the Center for BioDynamics, Boston University. The research of TK was supported in part by NSF Grant DMS-0072596.

1.5 References

[1] Andronov A and Leontovich E 1939 Some cases of the dependence of limit cycles upon parameters *Uch Zap Gork Univ* **6** 3–24 (in Russian)

[2] Arnold V I 1972 Lectures on bifurcations in versal families *Russ Math Surveys* **27** 54–123

[3] Av-Ron E, Parnas H and Segel L A 1993 A basic biophysical model for bursting neurons *Biol Cybern* **69** 87–95

[4] Baer S M, Erneux T and Rinzel J 1989 The slow passage through a Hopf bifurcation: delay, memory effects, and resonance *SIAM J Appl Math* **49** 55–71

[5] Baer S M, Rinzel J and Carrillo H 1995 Analysis of an autonomous phase model for neuronal parabolic bursting *J Math Bio* **33** 309–333

[6] Bautin N 1949 *Behavior of Dynamical Systems near the Boundaries of Stability Regions* (Leningrad and Moscow: OGIZ GOSTEXIZDAT) (in Russian)

[7] Benoit E 1991 *Dynamic Bifurcations: Luminy 1990* Lect Notes Math **1493** (Berlin: Springer)

[8] Bertram R, Butte M J, Kiemel T and Sherman A 1995 Topological and phenomenological classification of bursting oscillations *Bull Math Bio* **57** 413–439

[9] Bogdanov R 1975 Versal deformations of a singular point in the plane in the case of zero eigenvalues *Func Anal Appl* **9** 144–145

[10] Bogdanov R 1976 Versal deformations of a singular point in the plane in the case of zero eigenvalues in *Proc of Petrovski Sem* **2** Moscow University 23–35 (in Russian); English translation in *Sel Math Sov* **1**(4) 373–388

[11] Broer H W, Huitema G B, Takens F and Braaksma B L J 1990 Unfoldings and Bifurcations of Quasi-periodic Tori *Memoirs AMS* **83** 421

[12] Broer H W, Huitema G B and Sevryuk M B *Quasi-periodic Tori in Families of Dynamical Systems: Order Amidst Chaos* Lect Notes Math **1645** (Berlin: Springer)

[13] Canavier C C, Clark J W and Byrne J H 1991 Simulation of the bursting activity of neuron R15 In *Aplysia*: role of ionic currents, calcium balance, and modulatory transmitters *J Neurophys* **66** 2107–2124

[14] Candelpergher B, Diener F and Diener M 1990 Retard a la bifurcation: du local au global In *Bifurcations of Planar Vector Fields: Luminy 1989* Lect Notes Math **1455** (Berlin: Springer) 1–19

[15] Chay T R 1986 On the effect of intracellular calcium-sensitive K^+ channel in the bursting pancreatic β-cell *Biophys J* **50** 765–777

[16] Chay T R and Cook D I 1988 Endogenous bursting patterns in excitable cells *Math Biosci* **90** 139–153

[17] Chay T R and Keizer J 1983 Minimal model for membrane oscillations in the pancreatic β-cell *Biophys J* **42** 181–190

[18] Chay T R and Keizer J 1985 Theory of the effect of extracellular potassium on oscillations in the pancreatic β-cell *Biophys J* **48** 815–827

[19] Chay T R and Rinzel J 1985 Bursting, beating, and chaos in an excitable membrane model *Biophys J* **47** 357–366

[20] Chow S-N, Li C and Wang D 1994 *Normal Forms and Bifurcations of Planar Vector Fields* (Cambridge: Cambridge University Press)

[21] Diener F and Diener M 1991 Maximal delay In *Dynamic Bifurcations: Luminy 1990* Benoit E (ed) Lect. Notes Math **1493** (Berlin: Springer) 71–86

[22] Dumortier F, Roussarie R and Sotomayor J 1991 Generic three-parameter families of planar vector fields, unfoldings of saddle, focus, and elliptic singularities with nilpotent linear parts In *Bifurcations of Planar Vector Fields: Nilpotent Singularities and Abelian Integrals* Dumortier F, Roussarie R, Sotomayor J and Zoladek H (eds) Lect Notes Math **1480** (Berlin: Springer) 1–164

[23] Ermentrout G B and Kopell N 1986 Parabolic bursting in an excitable system coupled with a slow oscillation *SIAM J Appl Math* **46** 233–253

[24] Gavrilov N K 1978 On some bifurcations of an equilibrium with one zero and a pair of pure imaginary roots In *Methods of Qualitative Theory of Differential Equations* (Gorki: Gorki University Press) 33–40 (in Russian)

[25] Gavrilov N K 1980 On bifurcations of an equilibrium with two pairs of pure imaginary roots In *Methods of Qualitative Theory of Differential Equations* (Gorki: Gorki University Press) 17–30 (in Russian)

[26] Golubitsky M and Schaeffer D 1985, *Singularities and Groups in Bifurcation Theory I* Applied Mathematical Sciences series **51** (New York: Springer)

[27] Golubitsky M, Stewart I and Schaeffer D 1988 *Singularities and Groups in Bifurcation Theory II* Applied Mathematical Sciences series **69** (New York: Springer)

[28] Golubitsky M and Stewart I 2001 *The Symmetry Perspective* submitted

[29] Guckenheimer J 1981 On a codimension two bifurcation In *Dynamical Systems and Turbulence: Warwick 1980* Rand D A and Young L-S (eds) Lect Notes Math **898** (Berlin: Springer) 99–142

[30] Guckenheimer J and Holmes P 1990 *Nonlinear Oscillations, Dynamical Systems and Bifurcations of Vector Fields* Revised and corrected reprint of the 1983 original (Berlin: Springer)

[31] Guckenheimer J, Gueron S and Harris-Warrick R M 1993 Mapping the dynamics of a bursting neuron *Phil Trans Roy Soc Lond* **341** 345–359

[32] Hopf E 1942 Abzweigung einer periodischen Lösung von einer stationaren Lösung eines Differentialsystems *Berlin Math-Phys Kl Sachs: Acad Wiss Leipzig* **94** 1–22

[33] Hoppensteadt F C and Izhikevich E M 1997 *Weakly Connected Neural Networks* (Berlin: Springer)

[34] Hayes M G 1999 *Geometric analysis of delayed bifurcations* PhD-thesis Boston University

[35] Iooss G and Pérouème M C 1993 Perturbed homoclinic solutions in reversible 1:1 resonance vector fields *J Diff Eqs* **102** 62–88

[36] Izhikevich E 2000 Subcritical elliptic bursting of Bautin type *SIAM J Appl Math* **60** 503–535

[37] Izhikevich E 2000 Neural excitability, spiking and bursting *Int J Bif Chaos* **10** 1171–1266

[38] Keener J 1981 Infinite period bifurcation and global bifurcation branches *SIAM J Appl Math* **41** 127–144

[39] Kuznetsov Y A 1995 *Elements of Applied Bifurcation Theory* Applied Mathematical Sciences series **112** (Berlin: Springer)

[40] Langford W F 1979 Periodic and steady mode interactions lead to tori *SIAM J Appl Math* **37** 22–48

[41] Marsden J and McCracken M 1976 *The Hopf Bifurcation and Its Applications* (Berlin: Springer)

[42] Neihstadt A I 1987 Persistence of stability loss for dynamical bifurcations I *Diff Eq* **23** 1385–91

[43] Neihstadt A I 1988 Persistence of stability loss for dynamical bifurcations II *Diff Eq* **24** 171–196

[44] Pernarowski M 1994 Fast subsystem bifurcations in a slowly-varying Lienard system exhibiting bursting *SIAM J Appl Math* **54** 814–832

[45] Pernarowski M, Miura R M and Kevorkian J 1992 Perturbation techniques for models of bursting electrical activity in pancreatic β-cells *SIAM J Appl Math* **52** 1627–1250

[46] Pinsky R F and Rinzel J 1994 Intrinsic and network rhythmogenesis in a reduced Traub model for CA3 neurons *J Comp Neurosci* **1** 39–60

[47] Rhodes P A and Gray C M 1994 Simulations of intrinsically bursting neocortical pyramidal neurons *Neural Comp* **6** 1086–1110

[48] Rinzel J 1978 Repetitive activity and Hopf bifurcation under stimulation for a simple FitzHugh-Nagumo nerve conduction model *J Math Bio* **5** 363–382

[49] Rinzel J 1981 Models in neurobiology In *Nonlinear Phenomena in Physics and Biology* Enns R H, Jones B L, Miura R M and Rangnekar S S (eds) (New York: Plenum) 347–367

[50] Rinzel J 1985 Bursting oscillation in an excitable membrane model In *Ordinary and Partial Differential Equations* Sleeman B D and Jarvis R D (eds) Lect Notes Math **1151** (Berlin: Springer) 304–316

[51] Rinzel J 1987 A formal classification of bursting mechanisms in excitable systems In *Mathematical Topics in Population Biology, Morphogenesis and Neurosciences* Teramoto E and Yamaguti M (eds) Lect Notes Biomath **71** (Berlin: Springer) 267–281

[52] Rinzel J 1987 A formal classification of bursting mechanisms in excitable systems In *Proc Int Cong Math 1987* Gleason A M (ed) (Providence: American Mathematical Society) 1578–1593

[53] Rinzel J and Ermentrout G B 1989 Analysis of neural excitability and oscillations In *Methods in Neuronal Modeling: From Synapses to Networks* Koch C and Segev I (eds) (Cambridge: MIT Press) 135-169

[54] Rinzel J and Lee Y S 1986 On different mechanisms for membrane potential bursting In *Nonlinear Oscillations in Biology and Chemistry* Othmer H G (ed) Lect Notes Biomath **66** (Berlin: Springer) 19–33

[55] Rinzel J and Lee Y S 1987 Dissection of a model for neuronal parabolic bursting *J Math Bio* **25** 653–675

[56] Rubin J E and Terman D 1999 Geometric singular perturbation analysis of neuronal dynamics In *Handbook of Dynamical Systems III: Toward Applications* Takens F (ed) to appear

[57] Rush M E and Rinzel J 1994 Analysis of bursting in a thalamic neuron model *Bio Cybern* **71** 281–291

[58] Schecter S 1987 The saddle-node separatrix-loop bifurcation *SIAM J Math Anal* **18** 1142–1156

[59] Sherman A, Rinzel J and Keizer J 1988 Emergence of organized bursting in clusters of pancreatic β-cells by channel sharing *Biophys J* **54** 411–425

[60] Soto-Treviño C, Kopell N and Watson D 1996 Parabolic bursting revisited *J Math Bio* **35** 114–128

[61] Su J 1993 Delayed oscillation phenomena in the FitzHugh-Nagumo equation *J Diff Eqs* **105** 180–215

[62] Su J 1997 Effects of periodic forcing on delayed bifurcations *J Dyn Diff Eqs* **9** 561–625

[63] Takens F 1973 Unfoldings of certain singularities of vector fields: generalized Hopf bifurcations *J Diff Eqs* **14** 476–493

[64] Takens F 1974 Singularities of vector fields *Pub Math IHES* **43** 47–100

[65] Takens F 1976 Constrained equations: a study of implicit differential equations and their discontinuous solutions In *Structural Stability, the Theory of Catastrophes, and Applications in the Sciences* Hilton P (ed) Lect Notes Math **525** (Berlin: Springer) 143–234

[66] Terman D 1991 Chaotic spikes arising from a model of bursting in excitable membranes *SIAM J Appl Math* **51** 1418–1450

[67] de Vries G 1998 Multiple bifurcations in a polynomial model of bursting oscillations *J Nonlin Sci* **8** 281–316

[68] de Vries G and Miura R M 1998 Analysis of a class of models of bursting electrical activity in pancreatic β-cells *SIAM J Appl Math* **58** 607–635

[69] Wang X-J and Rinzel J 1994 Oscillatory and bursting properties of neurons In *The Handbook of Brain Theory and Neural Networks* Arbib M A (ed) (Cambridge: MIT Press) 686-691

[70] Zeeman E C 1973 Differential equations for heartbeat and nerve impulse In *Dynamical Systems* Peixoto M (ed) (New York: Academic Press) 683-741

[71] Zoladek H 1984 On the versality of a family of symmetric vector fields in the plane *Math USSR Sb* **48** 463–498
[72] Zoladek H 1987 Bifurcations of a certain family of planar vector fields tangent to axes *J Diff Eqs* **67** 1–55

Appendix: Case-by-case analysis of Hopf-steady state bursters of section 1.3.4

As stated in section 1.3.4, we present the case-by-case analysis of the unfolding (1.9) of the Hopf-steady state singularity in order to verify that there are indeed no new bursters found here. We follow the enumeration of the cases used in [20].

Case I. Under either forward or backward time, there is only one region in the (μ_1, μ_2) unfolding space in which there is a stable equilibrium point. Furthermore, this equilibrium disappears on the bifurcation curves that bound these regions, and there are no other stable invariant sets. In fact, most of the other invariant sets are saddle periodic orbits in the 3-D system. Hence, no bursting is observed with paths of the form (1.1).

Case II. All paths must avoid regions IIIa and IIIb in (1.9). Paths contained in the remaining regions exhibit either codimension-one bursting of the type created by nondegenerate Hopf bifurcations (see section 1.2) or the transition from a stable limit cycle to a stable two-torus (by crossing from region Ia or Ib into region II), which is precisely the new transition already described in section 1.3.4, or both.

Case III. In this case, we have already seen in section 1.3.4 that there is a new burster, bifurcation to a two-torus, that exists under time reversal in (1.9). To study the remaining possible bursters in this case, we begin by observing that all interesting paths must lie in the upper half of the parameter plane. However, in both forward and backward time, any such path other than that giving rise to two-torus bursting can only give rise to the bursting already found in the nondegenerate Hopf bifurcation, e.g., crossing between regions II and III or from II into IV via III.

Case IV. Again, here, all interesting paths must lie in the upper half of the (μ_1, μ_2) plane. There is one stable equilibrium there, but it can only disappear via a saddle-node bifurcation of equilibria or lose stability via a subcritical Hopf bifurcation. Hence, there is no bursting.